

Experimental realization of amorphous two-dimensional XY magnetsA. Liebig,^{1,2} P. T. Korelis,² Martina Ahlberg,² and B. Hjörvarsson²¹*Institute of Physics, Chemnitz University of Technology, D-09107 Chemnitz, Germany*²*Department of Physics and Astronomy, Uppsala University, Box 516, SE-751 20 Uppsala, Sweden*

(Received 4 March 2011; revised manuscript received 11 June 2011; published 19 July 2011)

The temperature dependence of the magnetization of thin amorphous $\text{Fe}_{89}\text{Zr}_{11}/\text{Al}_{78}\text{Zr}_{22}$ layers was investigated. Dimensionality analysis of the ferromagnetic transition of 15 Å thick layers yielded critical exponents characteristic of the 2D XY (planar rotor) model. Above the ordering temperature significant polarizability with an applied field is observed, due to the existence of large-scale magnetic correlations, of which the extent and origin have been determined.

DOI: [10.1103/PhysRevB.84.024430](https://doi.org/10.1103/PhysRevB.84.024430)

PACS number(s): 75.50.Kj, 75.40.-s, 75.70.-i, 64.60.F-

I. INTRODUCTION

Experimental realization of different universality classes is an important contribution to our understanding of the conceptual framework of phase transitions.¹⁻³ In this perspective, the two-dimensional Heisenberg and XY systems represent an important case, due to the subtle impact of finiteness on the presence of long-range order. In the thermodynamic limit, absence of long-range order is expected at any finite temperature, as famously proven in the Mermin-Wagner theorem.⁴ The theorem is valid in the thermodynamic limit, which implies infinite extension in two dimensions. When the size of a 2D XY magnet is limited, magnetic ordering is possible at finite temperatures and the order-disorder transition exhibits a well-defined universal behavior with a designated exponent.⁵ For structurally disordered magnets, our understanding is still less developed. Both exchange constants and magnetic anisotropy can vary substantially, which results in a rich variety of magnetic structures in bulk materials.^{6,7} The combined effect of confinement and structural disorder on the magnetic ordering is almost unknown. Exploration of the effect of confinement is therefore of major importance for establishing better understanding of the nature and stability of the magnetic ordering of structurally disordered materials.

The presence of anisotropy can affect the effective exponent in structurally ordered 2D magnets.⁸ In disordered systems, the effect of small random anisotropy (or random field) can even obstruct ferromagnetic order in four or less spatial dimensions.⁹ The magnetic order can be restored by the presence of additional global anisotropy in both 2D and 3D magnets.^{10,11} Thus, the magnetic anisotropy is an important parameter when considering the dimensionality aspects of structurally disordered magnets.

The magnetic properties of bulklike amorphous FeZr are well known.⁷ A transition to a re-entrant spin glass phase occurs at a temperature (T_{RE}) below the Curie temperature (T_C). T_{RE} decreases with increasing Zr concentration and at 11 at.% Zr the re-entrant state is practically suppressed.¹² At these Zr concentrations, the orbital contribution to the moment in Fe is close to zero, giving rise to effective decoupling of the magnetization and the structure.¹³ The growth of amorphous FeZr layers is established¹⁴ as well as the growth of FeZr/AlZr multilayers.¹⁵ Here, we will use $\text{Fe}_{89}\text{Zr}_{11}/\text{Al}_{78}\text{Zr}_{22}$ multilayers, in which the magnetic layers are decoupled, to address the behavior of thin $\text{Fe}_{89}\text{Zr}_{11}$ layers in the vicinity of the ferromagnetic transition.

II. EXPERIMENTAL DETAILS

The samples were deposited at room temperature in an ultrahigh vacuum system by dc magnetron sputtering. The argon pressure used was 0.4 Pa. The alloys were codeposited from elemental targets, and their composition was verified using Rutherford backscattering spectrometry. The substrates were Si(111) $1 \times 1 \text{ cm}^2$ wafers with a natural oxide layer. To ensure amorphous growth of the $\text{Fe}_{89}\text{Zr}_{11}$ layers, 60-Å-thick $\text{Al}_{78}\text{Zr}_{22}$ buffer layers were used.¹⁵ The multilayer samples were grown with 12 repetitions and all samples were capped with an aluminum layer to prevent oxidation.

A Quantum Design Magnetic Property Measurement System SQUID VSM magnetometer, which combines the measurement principle of a vibrating sample magnetometer with a superconducting quantum interference device (SQUID) sensor, was used for determining the absolute magnetization and the high field response of the samples. Large superconducting magnets, however, also show some hysteresis effects themselves due to magnetic flux frozen in the superconducting coil. High-resolution/low-field measurements were therefore performed using the magneto-optical Kerr effect, as described in Ref. 16. The magnetic field was generated by a pair of Helmholtz coils, the field amplitude was 70 Oe ($5.57 \times 10^3 \text{ A/m}$), and it alternated at 5 Hz. Hysteresis loops were continuously recorded while the temperature was varied with a heating rate of 0.2 K/min. Measurements recorded during 30 s were averaged to give one final hysteresis loop. The remanent magnetization as a function of temperature was extracted from this series of hysteresis loops.

III. RESULTS AND DISCUSSION

The T_C for a 300-Å $\text{Fe}_{89}\text{Zr}_{11}$ layer was determined to be 214 K, which is consistent with the literature values for bulk, which are in the range 210 to 240 K.^{7,17} T_C is strongly dependent on the thickness of the magnetic layer and a 15-Å $\text{Fe}_{89}\text{Zr}_{11}$ layer has a T_C of around 150 K. The use of multilayered stack to enhance the magnetic signal relies on the absence of interlayer exchange coupling (IEC). In the presence of IEC, both the ordering temperature and the exponent are affected.¹⁸ The coupling strength scales as d^{-n} , where d is the thickness of the spacer layer and n is a constant (typically in the range 2–3). Thus by comparing the ordering temperature of samples with different thicknesses of the $\text{Al}_{78}\text{Zr}_{22}$ layer, one can establish the presence or

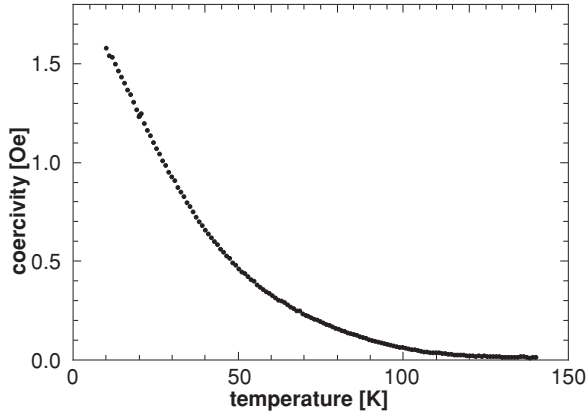


FIG. 1. Temperature dependence of the coercivity.

absence of IEC. The ordering temperature was found to be independent of the $\text{Al}_{78}\text{Zr}_{22}$ thickness, in the range 25 to 45 Å, proving a negligible IEC for these thicknesses. The absence of IEC across AlZr amorphous layers has also been confirmed in $\text{Fe}_{24}\text{Co}_{68}\text{Zr}_8/\text{Al}_{70}\text{Zr}_{30}$ trilayers, using ferromagnetic resonance.¹⁹ Based on these considerations we conclude that a multilayer with 15 Å thick magnetic layers and 45 Å thick interlayers can be treated as a sum of the contribution from independent layers. We therefore focus our attention on the magnetic properties of a $\text{Fe}_{89}\text{Zr}_{11}[15]/\text{Al}_{78}\text{Zr}_{22}[45]$ sample in the remainder of the communication.

The coercivity of $\text{Fe}_{89}\text{Zr}_{11}[15]/\text{Al}_{78}\text{Zr}_{22}[45]$ multilayers is small at all temperatures, as seen in Fig. 1. Thus, a full magnetization loop is obtained at relatively small fields. Furthermore, substantial changes in the magnetization are observed with small changes in the external field, as seen in Fig. 2. The strong field dependence of the magnetization below the ordering temperature hints toward the presence of a noncollinear contribution to the magnetization. Above the ordering temperature, the field dependence is markedly changed for a reason that is discussed below.

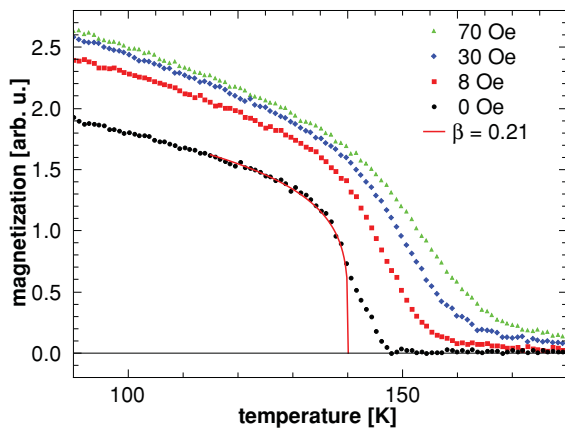


FIG. 2. (Color online) Temperature-dependent magnetization at different applied fields (MOKE data). A magnetization tail appears in measurements with an applied field. Also shown is the power law fit for $\beta = 0.21$.

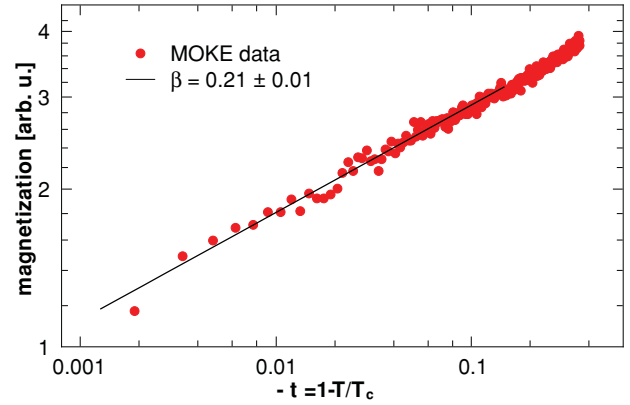


FIG. 3. (Color online) Fit of the zero-field magnetization curve with a power law in a double-logarithmic plot.

Close to T_C , the zero-field magnetization generally follows a power-law behavior:

$$M(T) = (1 - T/T_C)^\beta = (-t)^\beta, \quad (1)$$

where t is the reduced temperature. The critical exponents β and the T_C were determined by a direct fit of the magnetization with Eq. (1). The tail in the magnetization is caused by finite-size effects and could not be captured by a fit where Eq. (1) is convoluted with a Gaussian distribution of T_C . A fixed Curie temperature produces better fit quality over a larger temperature range. This effect is discussed further below. The T_C of 140.1 ± 1 K was used to plot the magnetization and reduced temperature on a double-logarithmic scale (Fig. 3) and β was extracted as the slope in the interval $10^{-3} \leq t \leq 10^{-1}$. Both the direct and linear fits resulted in a β value of 0.21 ± 0.01 . The value of the exponent verges on the universal value of 0.23 for the 2D XY model.^{5,8,20}

A 2D XY system is, in the finite-size limit, characterized by the Curie temperature T_C and two additional critical temperatures: the Kosterlitz-Thouless temperature, T_{KT} , and the finite-size shifted KT temperature, T^* .¹ T_C , however, is not as well defined as in other magnetic systems, and even theoretical models show a seemingly smeared transition.⁵ We follow here the definition of Bramwell and Holdsworth,⁵ who define T_C as the temperature where the correlation length becomes equal to the system size. T^* can be identified as the temperature where the critical exponent associated with the magnetic isotherm takes on its universal value⁵ $\delta = 15$, and then T_{KT} can be calculated from the relationship:

$$\frac{T^* - T_{KT}}{T_C - T_{KT}} = \frac{1}{4}. \quad (2)$$

T_{KT} plays a role in the divergent characteristics of the magnetic correlation length, which is described by:

$$\xi \propto \exp \left[\frac{b}{(T/T_{KT} - 1)^{1/2}} \right], \quad (3)$$

where b is a nonuniversal dimensionless constant.²

The value of δ , obtained by fitting the magnetic isotherms as illustrated in Fig. 4, becomes equal to 15 at $T = 136.1 \pm 0.1$ K which is identified as T^* . This results in a Kosterlitz-Thouless temperature of 134.6 ± 0.1 K. At the Curie temperature, δ takes

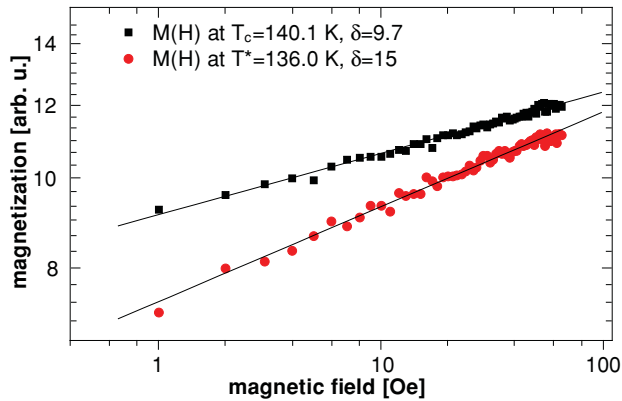


FIG. 4. (Color online) Double-logarithmic plot of the magnetic isotherms at T_C and T^* .

a value of 9.7, which clearly does not correspond to either the 2D Ising model ($\delta = 15$),²¹ or any 3D model ($\delta \approx 4.8$).^{22,23}

Above the Curie temperature, the spontaneous magnetization disappears. It is commonly stated that a ferromagnet becomes a paramagnet above T_C . If that were literally true, the response function above T_C would be²⁴ $M = N\mu L(x)$, where μ is the magnetic moment, N the number of magnetic moments per volume, $x = (\mu B)/(k_B T)$, and $L(x)$ is the Langevin function:

$$L(x) = \coth(x) - \frac{1}{x}. \quad (4)$$

Here, the magnetic response to an applied field is of the same order of magnitude, above and below T_C , which is inconsistent to a paramagnetic response (see Fig. 5). The magnetic correlations are therefore substantial, giving rise to large magnetic response, well above the ordering temperature. We can therefore gain some insight into the sizes and the length scales involved, assuming the magnetic correlations can be treated as macrospins with an average moment μ . Ignoring correlations between the macro spins, it is possible to estimate their size by fitting the field dependence of the magnetization, using Eq. (4). It has to be emphasized that this argument is semiquantitative, both due to the simplification in the model as well as the the uncertainty in the determination

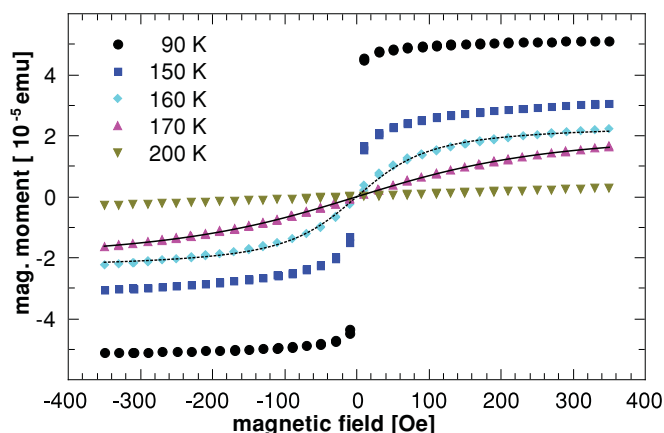


FIG. 5. (Color online) Magnetization at different temperatures (SQUID data). Langevin functions for 60×10^3 and 23.8×10^3 Bohr magnetons (for 160 K and 170 K, respectively) are also plotted.

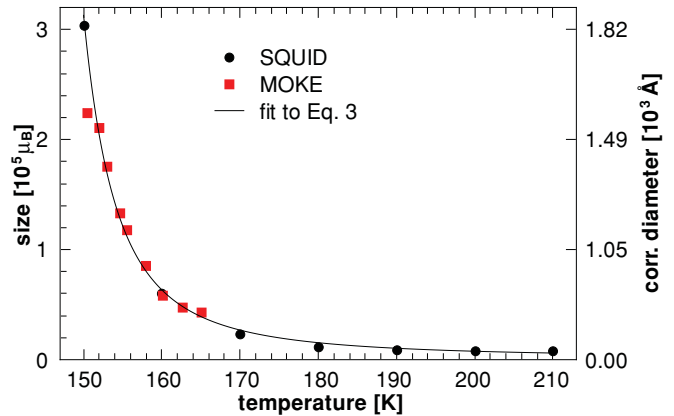


FIG. 6. (Color online) Number of correlated Bohr magnetons obtained from the Langevin fits at different temperatures, in units of moment size. On the right hand y axis is the diameter of the correlated regions. The solid line is a fit to Eq. (3) with $b = 1.22 \pm 0.05$.

of the atomic moment above the Curie temperature (which has here been assumed to be one-tenth of the moment below T_C).

Magnetization curves from both SQUID and MOKE measurements were used for this analysis. Since the maximum applied field in the MOKE setup is limited, meaningful data could only be extracted for a short temperature range just above T_C . Data points at higher temperatures, where larger fields were needed, were collected with the SQUID. The results from the fitting are plotted in Fig. 6 and around 160 K they overlap. When the temperature approaches T_C , the correlation length, together with the fluctuations, diverges and the Langevin description breaks down.

The size of the magnetic moment per iron atom in such multilayer structures is $0.85 \pm 0.09 \mu_B$ at 135 K.¹⁵ Using this as a reference point for that temperature on the magnetization versus temperature diagram, Fig. 2, we can estimate the effective moment at temperatures above T_C by extrapolation. This gives a moment in the order of $0.1 \mu_B$ per iron atom. Now the size of the correlated moment can be used to evaluate the diameter of the correlated regions. As seen in Fig. 6, regions with a diameter as large as 1000 \AA exist nearly 20 K above the transition temperature. The diameter of the correlated regions is proportional to the correlation length, at a given temperature. Using the Kosterlitz-Thouless temperature, determined above, the expression for the exponential decay of the correlation length with temperature [Eq. (3)] can be used to fit the data in Fig. 6. As seen in the figure, the data are accurately represented by the fitting, with $b = 1.22 \pm 0.05$. Fitting the data using T_{KT} as well as b as free parameters returns values with larger uncertainty, namely $T_{KT} = 132 \pm 4 \text{ K}$ and $b = 1.42 \pm 0.38$. The two sets of results completely overlap within the error bars.

A magnetization tail above T_C in response to small applied fields has also been observed in other two-dimensional systems (e.g., Ref. 3) and has been attributed to finite-size effects that broaden the ferromagnetic transition. This can, however, be interpreted within the framework of the 2D XY model without the need to assume a smeared phase transition due to ill-defined layer thickness or composition. Large magnetic correlations above T_C exist in a 2D XY system, since the correlation length has a finite, yet decaying, value. When a field is applied,

collections of locally correlated moments will align favorably with it, resulting in an increased magnetic response. This also explains the observation that the extent of the magnetization tail above the transition shows a dependence on the applied field strength, as seen in Fig. 2.

A comparison can be made between the thickness of the $\text{Fe}_{89}\text{Zr}_{11}$ layers with 2D XY behavior, in the amorphous multilayers investigated here, and crystalline Fe layers of the same dimensionality. 2D XY behavior is encountered for notably larger magnetic layer thickness for the amorphous films, as compared to Fe/V superlattices.²⁵ At the same time, the critical thickness for the onset of ferromagnetic ordering is much larger in, e.g., FeCoZr amorphous layers.²⁶ Thus, the physical extension of the layer and the effective magnetic thickness appears to be vastly different in this type of amorphous layers.

IV. CONCLUSIONS

A new class of magnetic materials, namely amorphous multilayers of $\text{Fe}_{89}\text{Zr}_{11}/\text{Al}_{78}\text{Zr}_{22}$, has been added to the experimentally verified cases of 2D XY systems. Furthermore, the extent of long-range magnetic correlations above the ferromagnetic transition, inherent features of this universality class, has been quantified. The existence of large dynamically correlated magnetic regions are not expected to be limited to thin amorphous films but should be viewed as a trademark of the 2D XY model.

ACKNOWLEDGMENT

Financial support from the Swedish Research Council (Vetenskapsrådet) and the Knut and Alice Wallenberg Foundation is gratefully acknowledged.

¹S. T. Bramwell, P. C. W. Holdsworth, and M. T. Hutchings, *J. Phys. Soc. Jpn.* **64**, 3066 (1995).

²J. Als-Nielsen, S. T. Bramwell, M. T. Hutchings, G. J. McIntyre, and D. Visser, *J. Phys. Condens. Matter* **5**, 7871 (1993).

³H. J. Elmers, J. Hauschild, G. H. Liu, and U. Gradmann, *J. Appl. Phys.* **79**, 4984 (1996).

⁴N. D. Mermin and H. Wagner, *Phys. Rev. Lett.* **17**, 1133 (1966).

⁵S. T. Bramwell and P. C. W. Holdsworth, *J. Phys. Condens. Matter* **5**, L53 (1993); *Phys. Rev. B* **49**, 8811 (1994).

⁶P. Tiberto, M. Baricco, E. Olivetti, and R. Piccin, *Adv. Eng. Mat.* **9**, 468 (2007).

⁷R. Garcia Calderon, L. Fernandez Barquin, S. N. Kaul, J. C. Gomez Sal, P. Gorria, J. S. Pedersen, and R. Heenan, *Phys. Rev. B* **71**, 134413 (2005).

⁸A. Taroni, S. T. Bramwell, and P. C. W. Holdsworth, *J. Phys. Condens. Matter* **20**, 275233 (2008).

⁹Y. Imry and S.-K. Ma, *Phys. Rev. Lett.* **35**, 1399 (1975).

¹⁰E. M. Chudnovsky, *J. Mag. Magn. Mat.* **40**, 21 (1983).

¹¹E. M. Chudnovsky, W. M. Saslow, and R. A. Serota, *Phys. Rev. B* **33**, 251 (1986).

¹²S. N. Kaul, *Curr. Sci.* **88**, 78 (2005).

¹³T. Hase, H. Raanaei, H. Lidbaum, C. Sanchez-Hanke, S. Wilkins, K. Leifer, and B. Hjörvarsson, *Phys. Rev. B* **80**, 134402 (2009).

¹⁴A. Liebig, P. T. Korelis, H. Lidbaum, G. Andersson, K. Leifer, and B. Hjörvarsson, *Phys. Rev. B* **75**, 214202 (2007).

¹⁵P. T. Korelis, A. Liebig, M. Björck, B. Hjörvarsson, H. Lidbaum, K. Leifer, and A. R. Wildes, *Thin Solid Films* **519**, 404 (2010).

¹⁶M. Pärnaste, M. van Kampen, R. Brucas, and B. Hjörvarsson, *Phys. Rev. B* **71**, 104426 (2005).

¹⁷A. R. Wildes, J. R. Stewart, N. Cowlam, S. Al-Heniti, L. F. Kiss, and T. Kemény, *J. Phys. Condens. Matter* **15**, 675 (2003).

¹⁸M. Marcellini, M. Pärnaste, B. Hjörvarsson, G. Nowak, and H. Zabel, *J. Mag. Magn. Mat.* **321**, 1214 (2009).

¹⁹Y. Fu, I. Barsukov, H. Raanaei, M. Spasova, J. Lindner, R. Meckenstock, M. Farle, and B. Hjörvarsson, *J. Appl. Phys.* **109**, 113908 (2011).

²⁰S. T. Bramwell and P. C. W. Holdsworth, *Appl. Phys. Lett.* **73**, 6096 (1993).

²¹L. Onsager, *Phys. Rev.* **65**, 117 (1944).

²²M. Hasenbusch, K. Pinn, and S. Vinti, *Phys. Rev. B* **59**, 11471 (1999).

²³M. Campostrini, M. Hasenbusch, A. Pelissetto, P. Rossi, and E. Vicari, *Phys. Rev. B* **65**, 144520 (2002).

²⁴S. Blundell, *Magnetism in Condensed Matter* (Oxford University Press, Oxford, UK, 2001).

²⁵M. Pärnaste, M. Marcellini, and B. Hjörvarsson, *J. Phys. Condens. Matter* **17**, L477 (2005).

²⁶M. Ahlberg, G. Andersson, B. Hjörvarsson, *Phys. Rev. B* **83**, 224404 (2011).